論文 / 著書情報
Article / Book Information

Title	Band-gap narrowing in α-(Cr_xFe_{1-x})₂O₃ solid-solution films
Authors	H. Mashiko,T. Oshima,A. Ohtomo
Citation	Applied Physics Letters, Vol. 99, ,
Pub. date	2011, 12
URL	http://scitation.aip.org/content/aip/journal/apl
Copyright	Copyright (c) 2011 American Institute of Physics

Band-gap narrowing in -(CrxFe1-x)2O3 solid-solution films

Hisanori Mashiko, Takayoshi Oshima, and Akira Ohtomo

Citation: Appl. Phys. Lett. **99**, 241904 (2011); doi: 10.1063/1.3669704
View online: http://dx.doi.org/10.1063/1.3669704
View Table of Contents: http://apl.aip.org/resource/1/APPLAB/v99/i24
Published by the American Institute of Physics.

Band-gap narrowing in α-$(Cr_xFe_{1-x})_2O_3$ solid-solution films

Hisanori Mashiko,[1] Takayoshi Oshima,[1] and Akira Ohtomo[1,2,a)]
[1]*Department of Applied Chemistry, Tokyo Institute of Technology, Tokyo 152-8552, Japan*
[2]*ALCA, Japan Science and Technology Agency, Tokyo 102-0076, Japan*

(Received 31 October 2011; accepted 23 November 2011; published online 13 December 2011)

We report on structural and optical properties for the (0001)-oriented α-$(Cr_xFe_{1-x})_2O_3$ ($0 \leq x \leq 1$) epitaxial films prepared on *c*-sapphire substrates by using pulsed-laser deposition. Pure corundum phase with atomically flat surface was obtained in the entire composition range. Optical absorption spectra for the films with $0.2 < x < 0.9$ showed a nearly constant band-gap (1.7 eV), which is narrower than those of α-Fe_2O_3 (2.1 eV) and α-Cr_2O_3 (3.0 eV). The result suggests that the band-gap narrowing arises from a type-II band alignment of these oxides and the fundamental band-gap lies between the Cr t_{2g} and O 2*p* occupied states and the Fe t_{2g}* empty state. © *2011 American Institute of Physics*. [doi:10.1063/1.3669704]

Aspects of visible light-driven photocatalysts have been widely studied to alleviate global warming upon development of sustainable energy production, including the water splitting and the artificial photosynthesis.[1,2] At present, the early transition-metal oxides with empty 3*d* states and wide band-gaps (e.g., TiO_2, Ta_2O_5, WO_6) are the most actively studied,[3] where tailoring their absorption bands to the sunlight spectrum often utilize the introduction of in-gap states by means of impurity doping (e.g., nitrogen-doped TiO_2).[4] The notion of band-gap engineering is an alternative approach and can be essentially applied to the late transition-metal oxides, where visible-light absorption naturally occurs owing to partially filled 3*d* states.[5] Due to the presence of complex intra-atomic *d*-*d* transitions, however, it remains unclear how the interatomic transitions are modulated in such solid-solutions. In addition, effects of the band modulation on absorption spectra may be hindered by unwanted factors such as defect-related in-gap absorption and optical scattering at the surface and grain boundaries. Therefore, one has to prepare thin single-crystalline samples to capture their intrinsic photoresponse.

In this study, we examine optical transitions in α-Fe_2O_3 based solid-solutions as a model system to explore the possibility for controlling band structures of transition-metal oxides suitable to visible light-driven photocatalysts. α-Fe_2O_3 is a stable compound in atmospheric environment and a promising photoanode material available from abundant minerals.[6,7] It is a charge transfer (CT) insulator with a band-gap (E_g) of 2.1 eV between occupied O 2*p* state and empty Fe 3*d* upper Hubbard band.[6,8,9] α-Cr_2O_3 is chosen as a counterpart material because of the absence of miscibility gap in binary phase diagram with α-Fe_2O_3.[10] It is known as a mixed CT and Mott-Hubbard insulator with $E_g = 3.3$ eV.[9,11,12] The α-Fe_2O_3/α-Cr_2O_3 heterostructure is known to have a type-II band alignment, where valence band maximum in α-Fe_2O_3 is lower than that of α-Cr_2O_3.[13] Band structures of these compounds are schematically illustrated in Fig. 1. The lowest transition level in their solid-solution is expected from occupied Cr t_{2g} and O 2*p* states to empty Fe t_{2g}* state, which is favorable to harvest a low-energy spectral region of the sunlight. Indeed we have observed red-shift of the absorption edge in our samples.

The α-$(Cr_xFe_{1-x})_2O_3$ thin films were grown on *c*-plane sapphire substrates by using an ultrahigh vacuum pulsed-laser deposition system and a KrF excimer laser. The substrates were annealed at 1100 °C for 3 h in air to obtain atomically flat surfaces. The film composition was varied with using sintered ceramics targets having different compositions of $x = 0$, 0.25, 0.50, 0.74, and 1. In addition, films with intermediate compositions were prepared by repeating alternate ablation of two neighboring targets. The best crystalline quality was reproducibly obtained under the following condition. The repetition and fluence of the laser were 10 Hz and 0.9 J/cm^2, respectively. Growth temperature was 740 °C and chamber pressure was a constant of 1 mTorr while flowing pure oxygen gas. Film thickness was regulated to be 40–80 nm. After the growth, the films were annealed at 1000 °C for 1 h in air. The film morphology and crystal structure were characterized by means of atomic force microscopy (AFM) and x-ray diffraction (XRD), respectively. The optical properties were investigated by UV-Vis-IR spectroscopy at room temperature. The film composition was analyzed for all the films by using a scanning electron microscopy equipped with an electron probe microanalyzer (EPMA). The composition of cations was confirmed to be identical to those of the targets and/

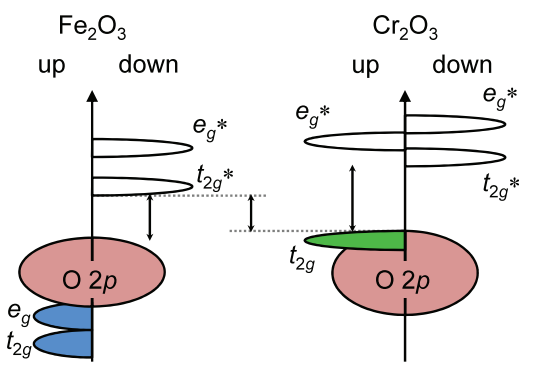

FIG. 1. (Color online) Schematic band structures of Fe_2O_3 and Cr_2O_3.

a)Electronic mail: aohtomo@apc.titech.ac.jp.

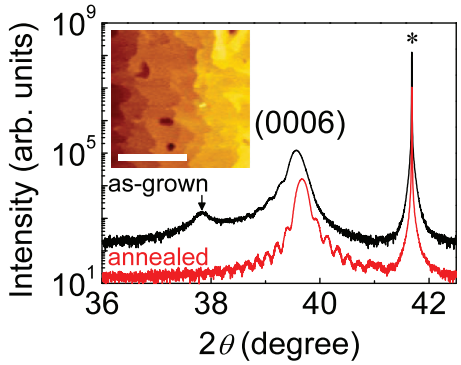

FIG. 2. (Color online) XRD patterns of the as-grown (black) and annealed (red) α-$CrFeO_3$ ($x = 0.5$) films near the (0006) reflection of α-Al_2O_3 substrate (*). Arrow indicates the (222) reflection of spinel phase. Inset depicts AFM image of the annealed film. Scale bar is 500 nm and color code is 5.4 nm in height.

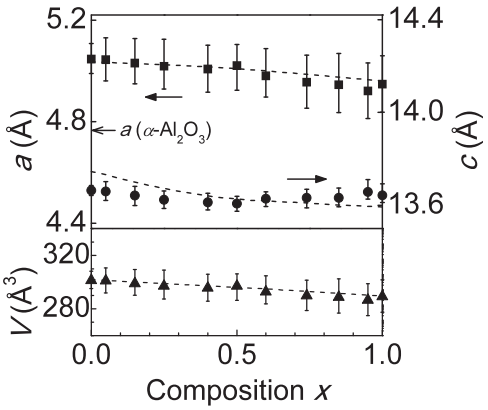

FIG. 3. Lattice parameters (top) and unit cell volume V (bottom) as a function of composition. Error bars represent full width at half maximum of the (0006) and (10$\bar{1}$4) reflections. Dashed line refers as to values for powder samples taken from Ref. 14.

or the compositions deduced from ratios of deposition rates and number of laser pulses for one to another target (the intermediate compositions), regardless of growth condition.

All the films were epitaxially grown along the c-axis with a single domain ([11$\bar{2}$0] α-$(Cr_xFe_{1-x})_2O_3$//[11$\bar{2}$0] α-Al_2O_3), whereas some of the as-grown films indicated a secondary phase, which was identified as the (111)-oriented spinel structure. After the annealing, the spinel phase was completely transformed to the corundum phase as formal valence of Fe ions changed from 2+ to 3+. Representative result is shown in Fig. 2 for the α-$CrFeO_3$ ($x = 0.5$) film. The surface became atomically flat after the annealing as verified from clear Laue fringes, as well as the AFM image (shown in inset). The height of surface steps was 0.46–1.12 nm, corresponding to multiple layers of the charge neutral unit ($c/6 \sim 0.23$ nm). We emphasize that these features are essential to analyzing subtle difference in absorption spectra, making effects of interference and scattering negligible.

The a- and c- axes lattice parameters were evaluated from the (0006) and (10$\bar{1}$4) reflections. The composition dependence of lattice parameters is plotted in the top panel of Fig. 3. A good agreement with values for powder samples (broken lines adapted from Ref. 14) indicates that high-quality and relaxed films were obtained in the entire range of composition. As shown in the bottom panel of Fig. 3, unit cell volume systematically decreased as Cr content increased, which is consistent with difference in ionic radii of Fe^{3+} (0.645 Å) and Cr^{3+} (0.615 Å).[15]

Figure 4(a) shows absorption spectra of the α-$(Cr_xFe_{1-x})_2O_3$ films. We took the first and second derivatives of the spectra to identify individual absorption bands as apparent peaks and/or shoulders. Figure 4(b) represents a central result of this study: all traces for characteristic absorption bands indicate complicated composition dependencies beyond the extent that a compound semiconductor solid-solution indicates large bowing behavior. Moreover, the emergence of shoulders at approximately 1.8 eV (■) is consistent with the aforementioned type-II band alignment. Direct and indirect band-gaps of corresponding samples were evaluated to be 2.1 eV and 1.7 eV, respectively [See Fig. 4(c)], assuming the

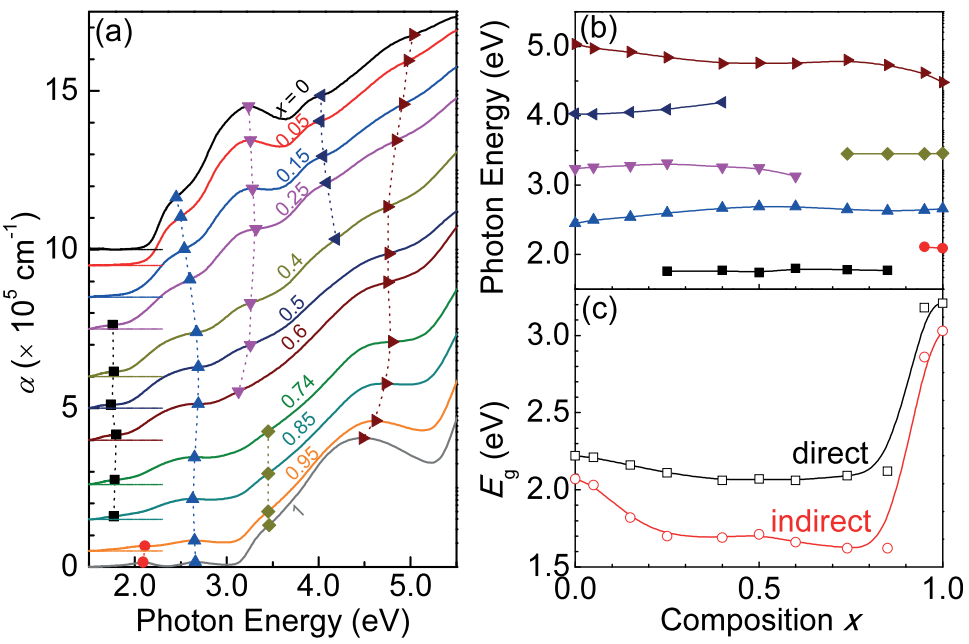

FIG. 4. (Color online) (a) Absorption spectra of the α-$(Cr_xFe_{1-x})_2O_3$ films. For clarity, each spectrum is offset with spacing scaled to the composition. (b) Composition dependence of the energy position for peaks and shoulders marked by different symbols in (a). (c) Composition dependence of the band-gap.

following relation: $\alpha h\nu \propto (h\nu - E_g)^n$ (Ref. 16), where α and $h\nu$ are absorption coefficient and photon energy, respectively, and n is either 2 (indirect) or 1/2 (direct). These values (indirect and direct E_g) are compared with those for α-Fe_2O_3 (2.1 eV and 2.2 eV) and α-Cr_2O_3 (3.0 eV and 3.2 eV).

Having established systematic change in absorption spectra, we discuss the origins of each transition. As for α-Fe_2O_3, fundamental absorption edge corresponds to a CT transition from O 2*p* state to Fe t_{2g}* states, which gradually evolves to the UV region showing a complex spectral shape. As for α-Cr_2O_3, discrete peaks at 2.1 eV (●) and 2.7 eV (▲) is attributed to *d-d* transitions as $^4T_{2g} \leftarrow {}^4A_{2g}$ and $^4T_{1g}$ (F) $\leftarrow {}^4A_{2g}$, respectively.[11,17] The CT transition from O 2*p* state gives a broad shoulder at 3.4 eV.[11] A maximum at 4.5 eV is assignable to a *d-d* transition as $^4T_{1g}$ (P) $\leftarrow {}^4A_{2g}$. For the solid-solution films, no apparent spectral weight transfer was observed, indicating significant overlaps of individual transitions. For example, one can see that the *d-d* transition of Cr^{3+} at 2.7 eV (▲) gradually shifts with increasing x and eventually merges into the CT band in α-Fe_2O_3. Systematic but independent variations in the transitions above 3 eV is presumably associated with change in the O 2*p* energy level.

Finally, we would like to discuss band-gap narrowing. According to literatures,[9,17,18] the absorption band at 1.8 eV corresponds to excitation of valence electrons at Cr t_{2g} and/or O 2*p* states to the empty Fe t_{2g}* state. This picture is further supported by a recent theoretical study based on density functional theory (DFT) calculations with a Hubbard *U*-term, which concludes that the band-gap of $CrFeO_3$ is reduced to 1.9 eV.[19] In order to develop active photocatalysts based on α-$(Cr_xFe_{1-x})_2O_3$, photocurrent measurements under visible light is now being conducted.

In summary, we have prepared high-quality (0001)-oriented α-$(Cr_xFe_{1-x})_2O_3$ solid-solution films by using pulsed-laser deposition. The absence of miscibility gap allows us to study systematic variations of structural and optical properties in the entire range of composition. From careful analyses of absorption spectra, we have found that fundamental band-gap is 1.7 eV in a composition range from $x = 0.2$ to 0.9. The lowest energy transition can be attributed to charge transfer from Cr t_{2g} and O 2*p* states to Fe t_{2g}* state. The use of high-quality epitaxial films will be a suitable approach to explore visible light-driven photocatalyst based on complex transition-metal oxides.

This work was partially supported by a grant from the Sumitomo Foundation. Authors thank Y. Wada and D. Mochizuki for assistance regarding EPMA.

[1]A. Fujishima and K. Honda, Nature **238**, 37 (1972).
[2]M. Grätzel, Acc. Chem. Res. **14**, 376 (1981).
[3]F. E. Osterloh, Chem. Mater. **20**, 35 (2008).
[4]R. Asahi, T. Morikawa, T. Ohwaki, K. Aoki, and Y. Taga, Science **293**, 269 (2001).
[5]T. Arima, Y. Tokura, and J. B. Torrance, Phys. Rev. B **48**, 17006 (1993).
[6]A. Kay, I. Cesar, and M. Grätzel, J. Am. Chem. Soc. **128**, 15714 (2006).
[7]J. Cao, T. Kako, N. Kikugawa, and J. Ye, J. Phys. D: Appl. Phys. **43**, 325101 (2010).
[8]S. U. M. Khan and J. Akikusa, J. Phys. Chem. B **103**, 7184 (1999).
[9]E. A. Moore, Phys. Rev. B **76**, 195107 (2007).
[10]A. Muan and S. Sōmiya, J. Am. Ceram. Soc. **43**, 204 (1960).
[11]K. W. Blazey, Solid State Commun. **11**, 371 (1972).
[12]T. Uozumi, K. Okada, A. Kotani, R. Zimmermann, P. Steiner, S. Hüfner, Y. Tezuka, and S. Shin, J. Electron Spectrosc. Relat. Phenom. **83**, 9 (1997).
[13]S. A. Chambers, Y. Liang, and Y. Gao, Phys. Rev. B **61**, 13223 (2000).
[14]T. Grygar, P. Bezdička, J. Dědeček, E. Petrovský, and O. Schneeweiss, Ceram.-Silikáty **47**, 32 (2003).
[15]R. D. Shannon, Acta Cryst. A **32**, 751 (1976).
[16]A. Hagfeldt and M. Grätzel, Chem. Rev. **95**, 49 (1995).
[17]S. Musić, M. Lenglet, S. Popović, B. Hannoyer, I. Czacó-Nagy, M. Ristić, D. Balzar, and F. Gashi, J. Mater. Sci. **31**, 4067 (1996).
[18]J. E. Jaffe, M. Dupuis, and M. Gutowski, Phys. Rev. B **69**, 205106 (2004).
[19]H. S. Nabi and R. Pentcheva, Phys. Rev. B **83**, 214424 (2011).